

## 一个新的粘液酸锰(II)配合物的合成、结构与性能研究

吕耀康 冯云龙\* 刘继伟 詹才宏 陈 静 王晓娟 蒋战果

(浙江师范大学物理化学研究所, 浙江省固体表面反应化学重点实验室, 金华 321004)

**摘要:** 合成了 1 个以粘液酸为配体的锰(II)配合物  $\text{Mn}[(\text{muc})(\text{H}_2\text{O})_3] \cdot \text{H}_2\text{O}$  (**1**), 并通过红外光谱, 元素分析, 热重分析和 X-射线单晶衍射对其进行了表征。配合物 **1** 由一维链组成, 其三维网络结构可以简化为 dia 拓扑。初步的电化学实验表明, 配合物 **1** 在电化学储能上有应用潜力, 可以作为氢氧化镍电极的添加剂。

**关键词:** 锰(II)配合物; 粘液酸; 晶体结构; 氢氧化镍电极; 添加剂

中图分类号: O614.7+11

文献标识码: A

文章编号: 1001-4861(2011)04-0791-06

## Synthesis, Crystal Structure and Properties of a New Manganese(II) Complex with Mucic Acid

LÜ Yao-Kang FENG Yun-Long\* LIU Ji-Wei ZHAN Cai-Hong

CHEN Jing WANG Xiao-Juan JIANG Zhan-Guo

(Zhejiang Key Laboratory for Reactive Chemistry on Solid Surfaces, Institute of Physical Chemistry,  
Zhejiang Normal University, Jinhua, Zhejiang 321004, China)

**Abstract:** A new manganese complex  $[\text{Mn}(\text{muc})(\text{H}_2\text{O})_3] \cdot \text{H}_2\text{O}$  (**1**) ( $\text{H}_2\text{muc}$ =mucic acid) has been synthesized and characterized by X-ray single-crystal diffraction, elemental analysis, IR spectrum, and thermogravimetry analysis. The structure of **1** is composed of 1D chains and further joined by hydrogen bonds to construct a 3D supramolecule structure. Preliminary electrochemical experiments indicated that as an additive on nickel hydroxide electrodes **1** could improve the electrochemical performance and has potential applications in electrochemical storage. CCDC: 720478.

**Key words:** manganese(II) complex; mucic acid; crystal structure; nickel hydroxide electrode; additive

## 0 Introduction

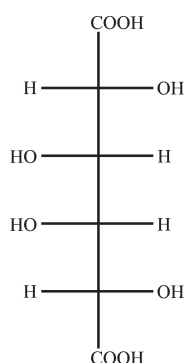
The rational design and synthesis of new metal-organic frameworks (MOFs) have undergone great efforts owing to their intriguing architectures and novel functionalities such as gas storage, luminescence, magnetism, ion exchanges, biology and catalysis, etc<sup>[1-11]</sup>. Mucic acid ( $\text{H}_2\text{muc}$ ) (Scheme 1) plays an important role in life science<sup>[12-13]</sup>. It is also a flexible multidentate

chelator that contains multiple hydroxyl groups along the carbon chain which may lead to a variety of coordinating modes and interesting structures. Recently, mucic acid is investigated as building blocks for metal-containing coordination networks because the surfaces of such complexes would be most unusual with regard to their high degree of hydroxylation<sup>[14-20]</sup>. Moreover, mucate complexes are readily renewable and biodegradable, which make them very attractive from the

收稿日期: 2010-09-01。收修改稿日期: 2010-12-27。

浙江省科技计划重点项目(No.2007C21174)资助。

\*通讯联系人。E-mail: sky37@zjnu.cn, Fax: 0086-0579-82282269

Scheme 1 Mucic acid ( $\text{H}_2\text{muc}$ )

environmental point of view, and if viable large-scale applications of such complexes were to be discovered and if sufficient demand were thereby generated the acid which is obtained from the oxidation of D-galactose could become very cheap to produce in bulk. In the past two decades, X-ray crystallographic studies of mucate complexes such as the mucates of Na, K<sup>[14]</sup>, Mg<sup>[15]</sup>, Ca, Ba<sup>[16]</sup>, Sr<sup>[17]</sup> and lanthanide<sup>[18-19]</sup> have been reported, but its transition metal complexes have not been well documented. Herein, we report the synthesis and structural characterization of a new complex,  $[\text{Mn}(\text{muc})(\text{H}_2\text{O})_3] \cdot \text{H}_2\text{O}$  (**1**).

## 1 Experimental

### 1.1 Materials and measurements

Spherical  $\beta\text{-Ni}(\text{OH})_2$  (containing Zn 3.0%, Co 1.5%) was purchased from Changsha Xinye Industrial Co., Ltd. All the starting materials were purchased commercially and used without further purification. IR spectrum was recorded on an FTIR-8700 spectrometer with KBr pellets in the range of  $4\,000\sim 400\text{ cm}^{-1}$ . Elemental analysis was performed on a EuroEA3000 elemental analyzer. Single-crystal X-ray diffraction measurement was carried out on a Bruker SMART APEX II CCD diffractometer with Mo  $K\alpha$  radiation ( $\lambda=0.071\,073\text{ nm}$ ). Thermogravimetric analysis was conducted on a Mettler-Toledo TGA/SDTA 851<sup>o</sup> instrument in  $25\sim 800\text{ }^\circ\text{C}$  ( $10\text{ }^\circ\text{C}\cdot\text{min}^{-1}$ ) range under oxygen atmosphere. Cyclic voltammetry (CV) was determined on CHI660C electrochemical analyzer (CH Instruments Corp. USA) at room temperature.

### 1.2 Synthesis of the complex **1**

$\text{Mn}(\text{CH}_3\text{CO}_2)_2 \cdot 4\text{H}_2\text{O}$  1.0 mmol (0.245 g) and mucic

acid 1.0 mmol (0.210 g) were dissolved in distilled water (40 mL). Addition of ethanol (30 mL) yielded a microcrystalline powder. The product was isolated by filtration and dried under vacuum at  $30\text{ }^\circ\text{C}$  for 12 h; yield 62.7%. Crystals suitable for X-ray diffraction studies were recrystallized from  $\text{H}_2\text{O}$ . Anal. Calcd. for  $\text{C}_6\text{H}_{16}\text{MnO}_{12}$ (%): C, 21.50; H, 4.78; found(%): C, 21.42; H, 4.60. IR (KBr,  $\text{cm}^{-1}$ ): 3 511(m), 3 473(m), 1 663(s), 1 654(s), 1 623(s), 863(w), 810(m), 752(m).

### 1.3 Preparations of complex **1** electrode

Powder of complex **1** and PTEE binder were mixed in a weight ratio of 95:5. And then the mixture was incorporated into a nickel foam (2 cm×1 cm) with spatula. The pasted nickel electrodes were dried at  $50\text{ }^\circ\text{C}$  and then pressed at a pressure of 15 MPa for 1 min.

### 1.4 Preparations of $\text{Ni}(\text{OH})_2$ electrode (**E0**)

$\beta\text{-Ni}(\text{OH})_2$  and PTEE binder were mixed in a weight ratio of 95:5. And then the mixture was incorporated into a nickel foam (2 cm×1 cm) with spatula. The pasted nickel electrodes were dried at  $50\text{ }^\circ\text{C}$  and then pressed at a pressure of 15 MPa for 1 min.

### 1.5 Preparations of complex **1**(7%)+ $\text{Ni}(\text{OH})_2$ electrode (**E1**)

Powder of complex **1**,  $\beta\text{-Ni}(\text{OH})_2$  and PTEE binder were mixed in a weight ratio of 7:88:5. mixture was incorporated into a nickel foam (2 cm×1 cm) with spatula. The pasted nickel electrodes were dried at  $50\text{ }^\circ\text{C}$  and then pressed at a pressure of 15 MPa for 1 min.

### 1.6 X-ray structure determination

The diffraction data for **1** was collected on a Bruker SMART APEX II diffractometer with Mo  $K\alpha$  radiation ( $\lambda=0.071\,073\text{ nm}$ ). Data intensity was corrected by Lorentz-polarization factors and empirical absorption. A total of 32 184 reflections were collected in the range of  $2.53^\circ \leq \theta \leq 27.32^\circ$ , of which 1 390 ( $R_{\text{int}}=0.062\,9$ ) were independent and 1 161 were observed ( $I>2\sigma(I)$ ). The structure was solved by direct methods and expanded using difference Fourier synthesis technique. All non-hydrogen atoms were refined anisotropically by the full matrix least-squares on  $F^2$ . The hydrogen atoms attached to carbon atoms were located by geometrical calculation, while those attached to oxygen were from the difference Fourier maps.

Calculations were performed with the SHELXS-97<sup>[21]</sup> and SHELXL-97<sup>[22]</sup> program packages. One of coordination water molecules and one lattice water molecule are disordered and their site occupancy factors refined to 0.5, respectively. Crystallographic data are summarized

in Table 1, selected bond lengths and angles are listed in Table 2, the hydrogen bond distances and bond angles are listed in Table 3, respectively.

CCDC: 720478.

**Table 1 Crystal data and summary of data collection for complex 1**

Empirical formula	C <sub>6</sub> H <sub>16</sub> MnO <sub>12</sub>	$D_c / (\text{g} \cdot \text{cm}^{-3})$	1.809
Formula weight	335.13	$\mu(\text{Mo } K\alpha) / \text{mm}^{-1}$	1.134
Crystalline system	Monoclinic	Crystal size / mm	0.12×0.08×0.07
Space group	$C2/c$	Reflections collected	32 184
$a / \text{nm}$	1.244 6(4)	Independent reflections	1 390
$b / \text{nm}$	1.107 1(5)	Observed reflections ( $I > 2\sigma(I)$ )	1 161
$c / \text{nm}$	0.946 5(6)	Parameters	120
$\beta / (^\circ)$	109.333(4)	$R / wR$ (observed data) ( $I > 2\sigma(I)$ )	0.067 4 / 0.153 4
$V / \text{nm}^3$	1.230 7(3)	$R / wR$ (all data)	0.087 0 / 0.170 4
$Z$	4	Goodness of fit on $F^2$	1.03
$F(000)$	692		

**Table 2 Selected bond lengths (nm) and angles ( $^\circ$ ) for complex 1**

Mn1-O2W	0.219 8(4)	Mn1-O1	0.227 7(3)	Mn1-O3	0.225 6(3)
Mn1-O1W	0.239 2(7)				
O2W#1-Mn1-O2W	177.3(2)	O1#1-Mn1-O1	76.89(17)	O2W#1-Mn1-O3#1	82.71(14)
O2W#1-Mn1-O1W	79.7(2)	O2W-Mn1-O3#1	96.50(14)	O2W-Mn1-O1W	97.6(2)
O2W#1-Mn1-O3	96.50(14)	O3#1-Mn1-O1W	75.6(3)	O2W-Mn1-O3	82.71(14)
O3-Mn1-O1W	71.0(3)	O3#1-Mn1-O3	146.11(17)	O1#1-Mn1-O1W	144.2(3)
O2W#1-Mn1-O1#1	91.65(14)	O1-Mn1-O1W	137.2(2)	O2W-Mn1-O1#1	90.46(14)
O2W#1-Mn1-O1W#1	97.6(2)	O3#1-Mn1-O1#1	68.87(12)	O2W-Mn1-O1W#1	79.7(2)
O3-Mn1-O1#1	144.79(12)	O3#1-Mn1-O1W#1	71.0(3)	O2W#1-Mn1-O1	90.46(14)
O3-Mn1-O1W#1	75.6(3)	O2W-Mn1-O1	91.65(14)	O1#1-Mn1-O1W#1	137.2(2)
O3#1-Mn1-O1	144.79(12)	O1-Mn1-O1W#1	144.2(3)		

Symmetry code: #1:  $1-x, y, 0.5-z$ .

**Table 3 Hydrogen bond distances and bond angles for 1**

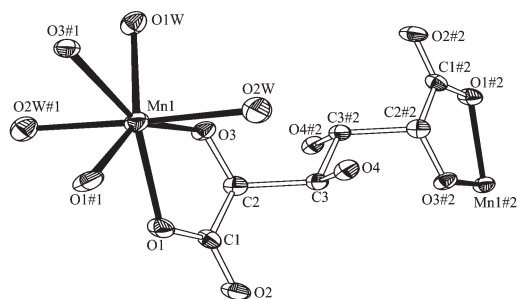
D-H...A	$d(\text{D-H}) / \text{nm}$	$d(\text{H}\cdots\text{A}) / \text{nm}$	$d(\text{D}\cdots\text{A}) / \text{nm}$	$\angle(\text{DHA}) / (^\circ)$
O3-H3...O2#1	0.084(2)	0.183(3)	0.264 2(5)	160(6)
O4-H4...O1#2	0.083(2)	0.192(2)	0.274 2(5)	171.(6)
O1W-H1W...O2#1	0.085(2)	0.202(3)	0.284 1(10)	162.(10)
O1W-H1WB...O3W	0.085(2)	0.155(9)	0.217 1(13)	127.(10)
O1W-H1WB...O3W#5	0.085(2)	0.187(2)	0.271 6(14)	178.(12)
O2W-H2WA...O4	0.084(5)	0.191(2)	0.274 4(5)	172.(5)
O2W-H2WB...O2#3	0.085(5)	0.198(5)	0.281 7(6)	173.(6)
O3W-H3WA...O2W#4	0.086(2)	0.219(5)	0.302 6(12)	165.(17)
O3W-H3WB...O1W	0.085(2)	0.160(14)	0.217 1(13)	121.(13)
O3W-H3WB...O1W#4	0.085(2)	0.222(12)	0.286 4(13)	132.(14)

Symmetry codes: #1:  $0.5-x, 0.5+y, 0.5-z$ ; #2:  $x, 1-y, 0.5+z$ ; #3:  $1-x, 1-y, 1-z$ ; #4:  $1-x, y, 0.5-z$ ; #5:  $1-x, y, z$ .

## 2 Results and discussion

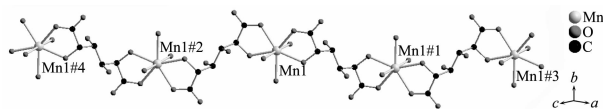
### 2.1 Crystal structure of complex 1

As shown in Fig.1, Each Mn(II) ion is coordinated by two carboxyl oxygen atoms, two  $\alpha$ -hydroxyl oxygen atoms from muc<sup>2-</sup> ligand and three waters in a distorted pentagonal bipyramid geometry. In this MnO<sub>7</sub> pentagonal bipyramid, O1, O3, O1#1, O3#1, O1W are situated in equator plane, O2W, O2W#1 are situated in axial positions of the pentagonal bipyramid. The Mn-O distances fall in the range from 0.219 8(4) to 0.239 2(7) nm, which are comparable to those in the previously reported complexes<sup>[23-27]</sup>. The muc<sup>2-</sup> ligand can be classed as  $\mu_2$ ,  $\kappa^4$ , and chelate the Mn(II) ions by two carboxyl oxygen donors and two  $\alpha$ -hydroxy groups, leading to an infinite 1D chain (Fig.2). Furthermore, the hydrogen bonds between the muc<sup>2-</sup> ligands and water molecules connect the neighboring chains to construct a 3D framework (Fig.3).



Symmetry codes: #1: 1-x, y, 0.5-z; #2: 0.5-x, 0.5-y, 1-z; Lattice water molecules and hydrogen atoms are omitted for clarity

Fig.1 Asymmetric unit of complex 1 with 30% probability displacement ellipsoids, showing the atom-labeling scheme

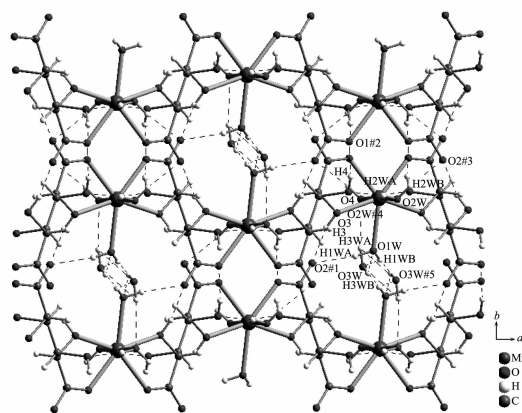


Symmetry codes: #1: 0.5-x, 0.5-y, z; #2: 0.5-x, 0.5-y, 1-z; #3: 1+x, y, 1+z; #4: 1+x, y, 1+z

Fig.2 1D chain structure of complex 1, all hydrogen atoms are omitted for clarity

Better insight of this architecture can be achieved by topology analysis. As shown in Fig.4a, each Mn(III) ion connects two muc<sup>2-</sup> ligands and two lattice water molecules through hydrogen bonds. If we define the Mn(II) ion as a single 4-connected node, the 3D

framework can be simplified as dia topology with Schlfli symbol of 6<sup>6</sup> (Fig.4b).



Symmetry codes: #1: 0.5-x, 0.5+y, 0.5-z; #2: x, 1-y, 0.5+z; #3: 1-x, 1-y, 1-z; #4: 1-x, y, 0.5-z; #5: 1-x, y, z

Fig.3 Packing diagram of the complex 1 view with extensive hydrogen-bonding interactions

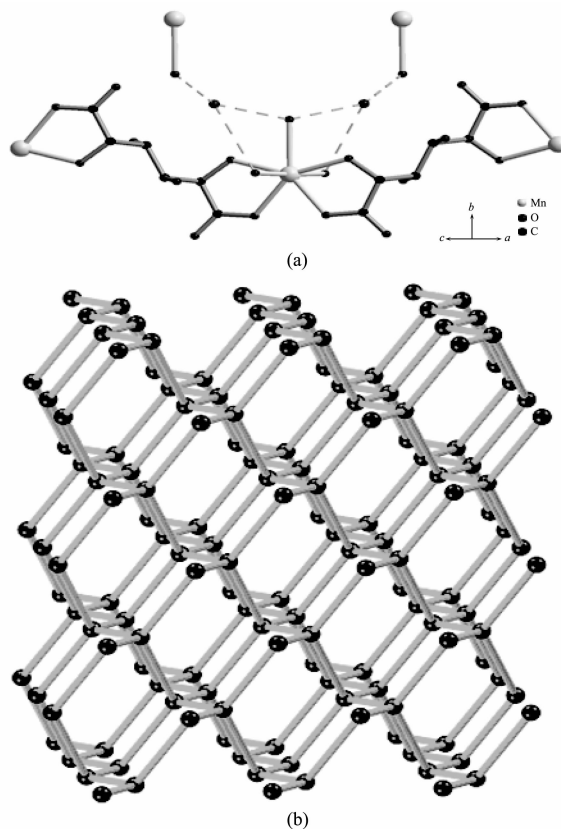


Fig.4 (a) View of the four-connected Mn(II) ion; (b) Schematic representation of the diamond topology

### 2.2 Thermogravimetry analysis of complex 1

The TGA curve of 1 indicates that the weight loss stages were completed at 313 °C, where the water

molecules and organic groups were burnt. The final residuals should be  $\text{MnO}_2$ , as the observed total weight loss of 74.48% is close to the theoretical one (74.05%).

### 2.3 Electrochemical performance

CV is a useful technique to evaluate the cycling performance of the electrodes. The experiments were carried out in a three-electrode mode cell at a scanning rate of  $100 \text{ mV} \cdot \text{s}^{-1}$ , in which Ni foil as the counter electrode,  $\text{Hg}/\text{HgO}$  as the reference electrode, and  $7 \text{ mol} \cdot \text{L}^{-1}$  KOH aqueous solution as the electrolyte. The cyclic voltammogram of complex **1** electrode is presented in Fig.5. There are one pair of redox peaks in the potential range from 200 to 400 mV. The peak potentials ( $E_{1/2} = (E_{\text{pc}} + E_{\text{pa}})/2$ ) are 310 mV, the potential difference ( $\Delta E_{\text{a,c}} = E_{\text{pa}} - E_{\text{pc}}$ ) are 83 mV, corresponding to a two-electron processes of Mn<sup>[28]</sup>. During the experiment, it can be observed that the electrolyte turned to brown, which indicates that complex **1** transformed to  $\text{Mn}(\text{OH})_2$  or  $\text{MnO}_2$  in the KOH aqueous.

$\text{Ni}(\text{OH})_2$  is used as positive electrode materials in Ni-based battery (Ni-MH, Ni-Fe, etc.), the good performance of  $\text{Ni}(\text{OH})_2$  is critical for battery<sup>[29-31]</sup>. It has been reported that the addition of inorganic materials<sup>[32-36]</sup> to  $\text{Ni}(\text{OH})_2$  can improve the capacity of the  $\text{Ni}(\text{OH})_2$  electrode. However, to the best of our knowledge, the effects of MOFs as additive on the electrochemical properties of nickel hydroxide electrodes has not been investigated. We used CV to evaluate the electrochemical performance of addition complex **1** to  $\beta\text{-Ni}(\text{OH})_2$ . For comparison, complex **1** (7%)+ $\text{Ni}(\text{OH})_2$  Electrode (E1) and  $\text{Ni}(\text{OH})_2$  Electrode (E0) were constructed by the same procedure. The typical CV curves of E1 and E0 are shown in Fig.6. It can be seen that there is only one anodic (oxidation) and one cathodic (reduction) peak on the CV curves for both samples in the range of scanning potentials employed. The anodic oxidation peak, which is associated with the conversion of nickel hydroxide to nickel oxyhydroxide, appears at about 664 mV for E0. Compared with the peak potential of E0, the oxidation peak for E1 (532 mV) shifted towards more negative potentials by about 132 mV. The reduction peaks, which are associated with the conversion of oxyhydroxide back to nickel hydroxide, appear at about

-2 mV and -124 mV for E0 and E1, respectively<sup>[32]</sup>. The potential difference between anodic and cathodic peak positions ( $\Delta E_{\text{a,c}}$ ) is used to estimate the reversibility of the electrode reaction<sup>[37-38]</sup>. The  $\Delta E_{\text{a,c}}$  value (408 mV) of E1 was smaller than that (662 mV) of E0, which indicated the reversibility of redox reaction for the E1 was notably better than E0. In all, the preliminary electrochemical experiment showed that the addition of complex **1** could improve the electrochemical performance of nickel hydroxide electrode and complex **1** might have potential application in electrochemical storage.

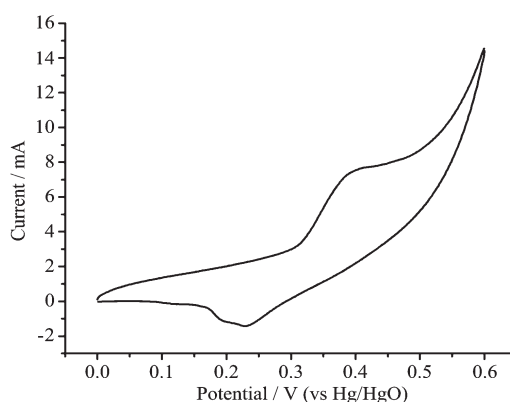


Fig.5 Cyclic voltammogram of complex **1**, electrode recorded at  $100 \text{ mV} \cdot \text{s}^{-1}$

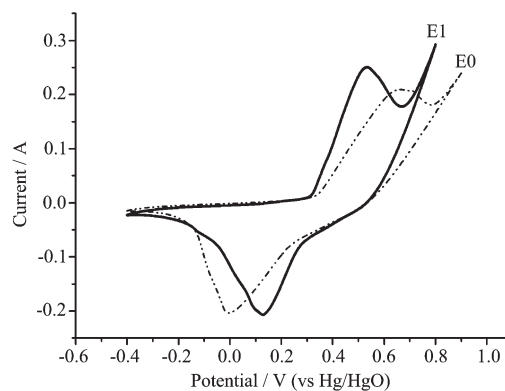


Fig.6 Cyclic voltammograms of complex **1** (7%) +  $\text{Ni}(\text{OH})_2$  electrode (E1) and  $\text{Ni}(\text{OH})_2$  electrode (E0) at scan rate of  $100 \text{ mV} \cdot \text{s}^{-1}$  in  $7 \text{ mol} \cdot \text{L}^{-1}$  KOH at room temperature

### 3 Conclusion

A new complex  $[\text{Mn}(\text{muc})(\text{H}_2\text{O})_3] \cdot \text{H}_2\text{O}$  (**1**) has been prepared and characterized. The structure of **1** is composed of 1D chains and the 3D framework constructed by hydrogen bonds can be simplified as dia topology. Preliminary electrochemical experiments



indicated that **1** could be used as an additive on nickel hydroxide electrodes and has potential applications in electrochemical storage.

## References:

- [1] Gao E Q, Bai S Q, Wang Z M, et al. *J. Am. Chem. Soc.*, **2003**, **125**:4984-4985
- [2] Ghosh A K, Ghoshal D, Zangrando E, et al. *Inorg. Chem.*, **2005**, **44**:1786-1793
- [3] Su C Y, Yang X P, Kang B S, et al. *Angew. Chem., Int. Ed.*, **2001**, **40**:1725-1728
- [4] Tian Y Q, Cai C X, Ji Y, et al. *Angew. Chem., Int. Ed.*, **2002**, **41**:1384-1386
- [5] Holliday B J, Mirkin C A. *Angew. Chem., Int. Ed.*, **2001**, **40**:2022-2043
- [6] Gianneschi N C, Masar M S III, Mirkin C A. *Acc. Chem. Res.*, **2005**, **38**:825-837
- [7] Bi W H, Cao R, Sun D F, et al. *Chem. Commun.*, **2004**:2104-2105
- [8] Chen W, Yuan H M, Wang J Y, et al. *J. Am. Chem. Soc.*, **2003**, **125**:9266-9267
- [9] He Y H, Feng Y L, Lan Y Z, et al. *Cryst. Growth Des.*, **2008**, **8**:3586-3594
- [10] Lü Y K, Zhan C H, Feng Y L. *CrystEngComm.*, **2010**, **12**:3052-3056
- [11] Lü Y K, Zhan C H, Jiang Z G, et al. *Inorg. Chem. Commun.*, **2010**, **13**:440-444
- [12] Anet E F L G, Reynolds T M. *Nature*, **1954**, **174**:930-
- [13] Wang W, Wan W, Stachiw A, et al. *Biochemistry*, **2005**, **44**:10751-10756
- [14] Taga T, Shimada T, Mimura N. *Acta Crystallogr. C*, **1994**, **50**:1076-1079
- [15] Sheldrick B, Mackie W. *Acta Crystallogr. C*, **1989**, **45**:1072-1073
- [16] Sheldrick B, Mackie W, Akrigg D. *Acta Crystallogr. C*, **1989**, **45**:191-194
- [17] Tian W, Cheng S, Yang L M, et al. *J. Inorg. Biochem.*, **2000**, **78**:197-204
- [18] Abrahams B F, Moylan M, Orchard S D, et al. *CrystEngComm*, **2003**, **5**:313-317
- [19] Wong K L, Law G L, Yang Y Y, et al. *Adv. Mater.*, **2006**, **18**:1051-1054
- [20] Lü Y K, Zhan C H, Chen J, et al. *Chin. J. Struct. Chem.*, **2010**, **29**:1483-1488
- [21] Sheldrick G M. *SHELXS-97, Program for Crystal Structure Solution*, University of Göttingen, Germany, **1997**.
- [22] Sheldrick G M. *SHELXL-97, Program for Crystal Structure Refinement*, University of Göttingen, Germany, **1997**.
- [23] Field L M, Lahti P M, Palacio F, et al. *J. Am. Chem. Soc.*, **2003**, **125**:10110-10118
- [24] Poulsen R D, Bentien A, Chevalier M, et al. *J. Am. Chem. Soc.*, **2005**, **127**:9156-9166
- [25] Lu W G, Gu J Z, Jiang L, et al. *Cryst. Growth Des.*, **2008**, **8**:192-199
- [26] Wang X W, Dong Y R, Zheng Y Q, et al. *Cryst. Growth Des.*, **2007**, **7**:613-615
- [27] Fettouhi M, Khaled M, Waheed A, et al. *Inorg. Chem.*, **1999**, **38**:3967-3971
- [28] Qu D Y, Conway B E, Bai L. *J. Appl. Electrochem.*, **1993**, **23**:693-706
- [29] Bode H, Dehmelt K, Kenntnis Z. *Electrochim. Acta*, **1966**, **11**:1079-1087
- [30] Naito K, Matsunami T, Okuno K, et al. *J. Applied Electrochemistry*, **1993**, **23**:1051-1055
- [31] Stuart T A, Hande A. *Journal of Power Sources*, **2004**, **129**:368-378
- [32] Soria M L, Chacon J, Hernandez J C. *Journal of Power Sources*, **2001**, **102**:97-104
- [33] LÜ Yao-Kang (吕耀康), FENG Yun-Long (冯云龙). *Chinese J. Inorg. Chem. (Wuji Huaxue Xuebao)*, **2009**, **25**:447-453
- [34] Liu H B, Xiang L, Jin Y. *Cryst. Growth Des.*, **2006**, **6**:283-286
- [35] Watanabe K, Kikuoka T, Kumagai N. *J. Appl. Electrochem.*, **1995**, **25**:219-226
- [36] Li W Y, Zhang S Y, Chen J. *J. Phys. Chem. B*, **2005**, **109**:14025-14032
- [37] Corrigan D A, Bendert R M. *J. Electrochem. Soc.*, **1989**, **136**:723-728
- [38] Wu Q D, Gao X P, Li G R, et al. *J. Phys. Chem. C*, **2007**, **111**:17082-17087